Oxygen-Transport Properties of Liquid-Crystalline Polyesters Based on 4,4′-Bibenzoic Acid

Y. S. Hu, H. P. Wang, D. A. Schiraldi, A. Hiltner, E. Baer

Department of Macromolecular Science and Engineering, Center for Applied Polymer Research, Case Western Reserve University, Cleveland, Ohio 44106–7202

Received 14 March 2006 ; accepted 28 April 2006
DOI 10.1002/app.26008
Published online in Wiley InterScience (www.interscience.wiley.com).

ABSTRACT: This study examined the oxygen-transport properties of aromatic liquid-crystalline (LC) polyesters of 4,4′-bibenzoic acid (BB) and an aliphatic diol. The effect of the spacer length was probed by the number of methylene groups in the diol being increased from 3 to 6. Parallel studies were performed on polymers in which the LC character was reduced or removed by copolymerization with 30 mol % nonmesogenic isophthalic acid (BB-30I) or by the replacement of BB with 4,4′-oxybis(benzoic acid) (OBB). The oxygen-transport properties were interpreted in terms of the solid-state structure as revealed by the thermal behavior and wide-angle X-ray diffraction. The strong odd–even effect of the spacer length that characterized the thermal transitions of the BB polyesters was weak or absent from the oxygen-transport properties when the effect of crystallinity was considered. Permeability and diffusivity tended to increase with the spacer length. The lower oxygen permeability of all the BB polyesters compared with that of the BB-30I copolyesters and the OBB polyesters was due primarily to lower oxygen solubility. The low solubility of the noncrystalline LC phase was ascribed to a smaller free-volume hole size and possibly to a lower free-volume hole density in comparison with an amorphous glass. The solubility of oxygen in the noncrystalline regions of the BB-30I copolyesters and in the amorphous OBB polyesters conformed to the relationship between the solubility and the glass-transition temperature previously established for amorphous and glassy aromatic polyesters. J Appl Polym Sci 105: 30–37, 2007

Key words: barrier; liquid-crystalline polymers (LCP); polyesters

INTRODUCTION

Thermotropic liquid-crystalline polymers (LCPs) are interesting as engineering plastics because of their low viscosity and ease of orientation, their high strength, and their good barrier performance. The extraordinarily low gas permeability of LCPs stems mainly from low solubility rather than from low diffusivity.[1–4] Previous studies of thermotropic liquid-crystalline (LC) polyesters based on 4,4′-bibenzoic acid (BB) and aliphatic diols have revealed a glassy LC state with a hole-free-volume intermediate between those of the permeable, amorphous glass and the impermeable, three-dimensional crystal.[5–9] In this interpretation, the LC order leads to inherently low gas solubility.

The LC polyesters prepared from BB and linear aliphatic diols can be produced in conventional polyester reactors and injection-molded. The polymers have good mechanical properties, high heat deflection temperatures, and excellent solvent resistance.[10] Their thermal stability is guaranteed up to 300°C.[11] These characteristics make the BB polyesters especially attractive for investigations of structure–property relationships of LCPs.[12–14] The biphenyl group is the mesogen and provides the linearity and symmetry that make possible the formation of smectic layers. The aliphatic diol provides a flexible spacer between the smectic layers. The length of the flexible spacer can be varied by changes in the number of methylene groups (n) in the diol. The transition temperatures of aliphatic bibenzoates show an odd–even oscillation, with higher temperatures observed for even-numbered spacers. The odd–even effect has been attributed to constraints on the arrangement of mesogenic groups when they are part of a polymer molecule.[11,15] The constraints are imposed by the conformation of the intervening aliphatic spacer. For odd values of n, the polymer chain tends to assume a conformation with two successive mesogenic groups tilted toward each other, forming the so-called smectic CA structure. The mesogenic groups in the polymers with even n values lie parallel to one another and form the smectic A structure.

This study examined the effect of the spacer length on the oxygen-transport properties of smectic BB polyesters. Poly(propylene 4,4′-bibenzoate) (PP3BB), poly(butylene 4,4′-bibenzoate) (PBBB), poly(pentamethylene 4,4′-bibenzoate) (PP5BB), and poly(hexa-

This article is dedicated to the memory of Professor Marian Kryszewski.

Correspondence to: A. Hiltner (pah6@case.edu).

Contract grant sponsor: KoSa.
Contract grant sponsor: Modern Controls, Inc.

methylene 4,4′-bibenzoate) (PHBB) with n values of 3, 4, 5, and 6, respectively, were chosen for comparison. Parallel studies were performed on polymers in which the LC character was reduced or eliminated. In one approach, the LC character was reduced by copolymerization with nonmesogenic isophthalic acid. A second approach employed polyesters based on 4,4′-oxybis(benzoic acid) (OBB). The oxygen-transport properties were interpreted in terms of the solid-state structure as revealed by thermal analysis and wide-angle X-ray diffraction (WAXD).

EXPERIMENTAL

The polymers were prepared by melt polymerization as described previously[6] and were supplied by KoSa (Spartanburg, SC) in the form of pellets. The chemical structure of the LC polyesters of BB and aliphatic diols was as follows:

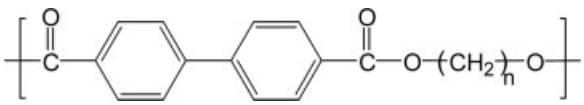

The polymers with *n* values of 3, 4, 5, and 6 were PP3BB, PBBB, PP5BB, and PHBB, respectively. The intrinsic viscosity of all the polyesters was between 0.6 and 0.8 dL/g at 25°C in a 1% w/w dichloroacetic acid solution.

Copolymers with 30 mol % BB replaced with isophthalic acid were also studied. The copolymers were identified by the name of the homopolymer followed by -30I, such as PBBB-30I, PP5BB-30I, and PHBB-30I. The randomization of the copolymers was virtually assured by the melt polymerization conditions that were used. The comonomer content was given as the reaction feed.

The polyesters based on OBB and aliphatic diols had the following chemical structure:

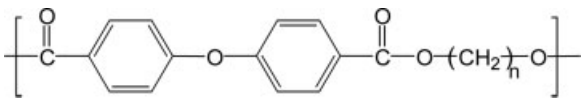

The polymers with *n* values of 2, 4, and 6 were designated PEOBB, PBOBB, and PHOBB, respectively.

The pellets were dried *in vacuo* for 24 h at a temperature between the ambient temperature and 80°C, depending on the comonomer content, and compression-molded between Kapton films in a press at a temperature between 150 and 320°C to obtain films 180–200 μm thick. Quenched films were transferred rapidly from the isotropic melt into iced water. It was not possible to quench PP3BB, PBBB, PP5BB, PHBB, PBBB-30I, and PHBB-30I into an amorphous glass because of the extremely rapid LC or crystalline transitions. Other polymers were quenched into an amorphous glass.

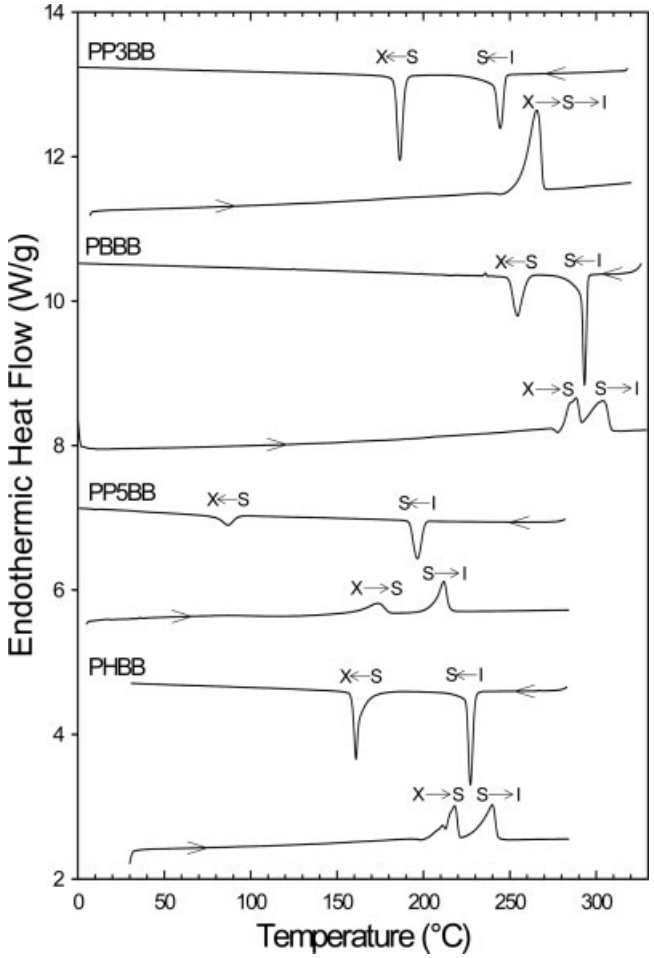

Figure 1 Thermograms of BB polyesters cooled from the isotropic melt and reheated at 10°C/min.

A thermal analysis was conducted under nitrogen with a PerkinElmer (Waltham, MA) DSC-7 calibrated with indium and tin. Heating and cooling thermograms were recorded at a scanning rate of 10°C/min from 0 to at least 30°C above the smectic–isotropic (S–I) transition.

WAXD patterns of the quenched films were obtained at the ambient temperature with a Rigaku (Woodland, TX) diffractometer in the transmission mode with a slit angle of 1/12°. To obtain the amount of the crystallinity, the area contributed by the crystalline peaks was divided by the total area under the WAXD curve. The amorphous baseline was approximated by a smooth curve that intersected as many valley points between the crystalline peaks as possible.

The density of the quenched films was measured at 23°C with a density gradient column constructed from an aqueous solution of calcium nitrate in accordance with ASTM D 1505 Method B. Small pieces of film (~ 25 mm^2) were placed in the column and allowed to equilibrate for 30 min before the measurements were taken.

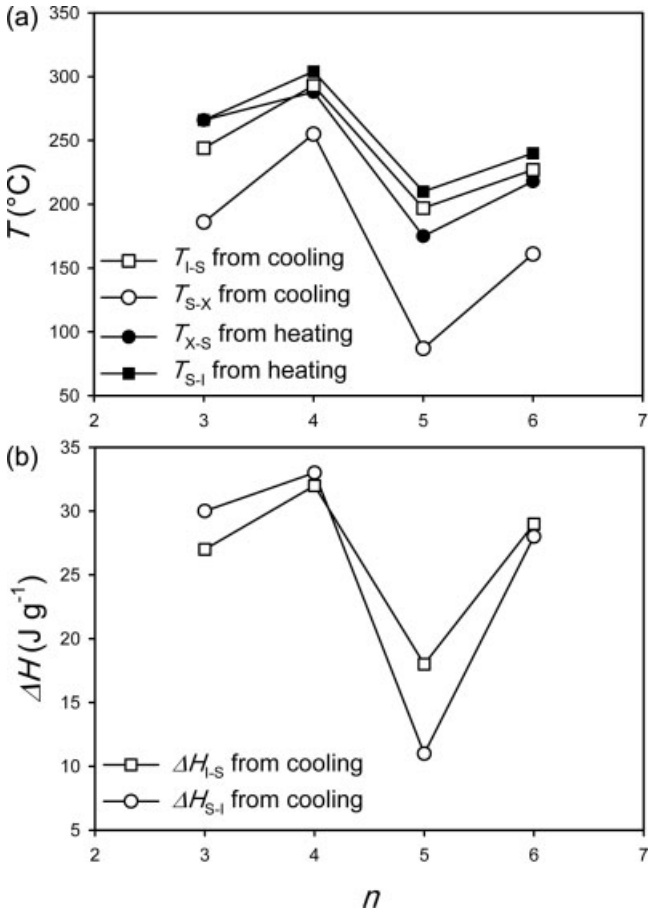

Figure 2 Effect of the spacer length on the thermal transitions of BB polyesters: (a) transition temperatures and (b) transition enthalpies.

Positron annihilation lifetime spectroscopy was performed with a conventional fast–fast coincidence system. The instrumentation and procedures for the data analysis were described previously.[16]

The oxygen flux [$J(t)$] at 23°C, 0% relative humidity, and 1 atm of pressure was measured with a Mocon (Minneapolis, MN) OX-TRAN 2/20. The instrument was calibrated with Mylar film (certified by the National Institute of Standards and Technology) of known oxygen-transport characteristics. The specimens were carefully conditioned as described previously[17] to obtain the non-steady-state $J(t)$ value from which the diffusivity parameter (D) was determined. To obtain D and to accurately determine the permeability parameter (P), the data were fit to the solution of Fick's second law with appropriate boundary conditions:

$$J(t) = \frac{Pp}{l}\left[1 + 2\sum_{n=1}^{\infty}(-1)^n \exp\left(-\frac{D\pi^2 n^2 t}{l^2}\right)\right] \quad (1)$$

where l is the average film thickness, p is the permeant gas pressure, and t is the time. l of each specimen was determined as $l = W(A\rho)^{-1}$, where W is the specimen weight, A is the specimen area, and ρ is the density. The solubility parameter (S) was calculated with the relationship $S = PD^{-1}$.

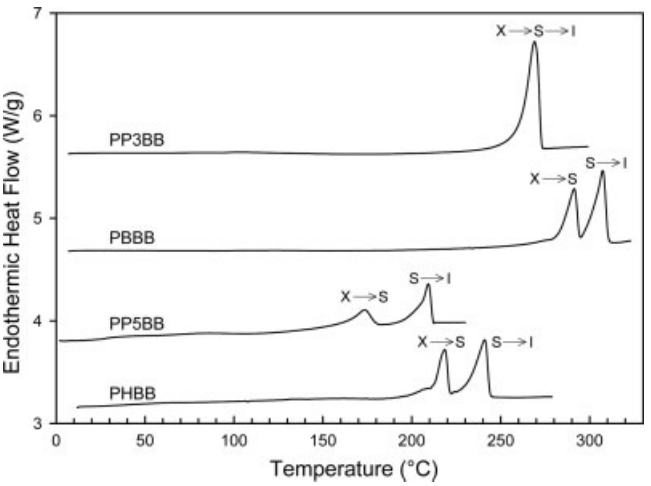

Figure 3 Heating thermograms of quenched BB polyester films.

RESULTS AND DISCUSSION

Thermal transitions

The thermograms of LC polyesters of BB and aliphatic diols in Figure 1 were obtained via cooling at a rate of 10°C/min followed by heating at a rate of 10°C/min. The interpretation of the thermograms follows previous reports.[10–15,18] All cooling curves exhibited a sharp exothermic peak corresponding to the isotropic–smectic transition (I–S) at T_{I-S} with an enthalpy of ΔH_{I-S}, which was followed by an exothermic smectic–crystalline (S–X) transition at T_{S-X} with an enthalpy of ΔH_{S-X}. The subsequent heating curves usually showed two major peaks corresponding to the crystalline–smectic (X–S) transition at T_{X-S} with an enthalpy of

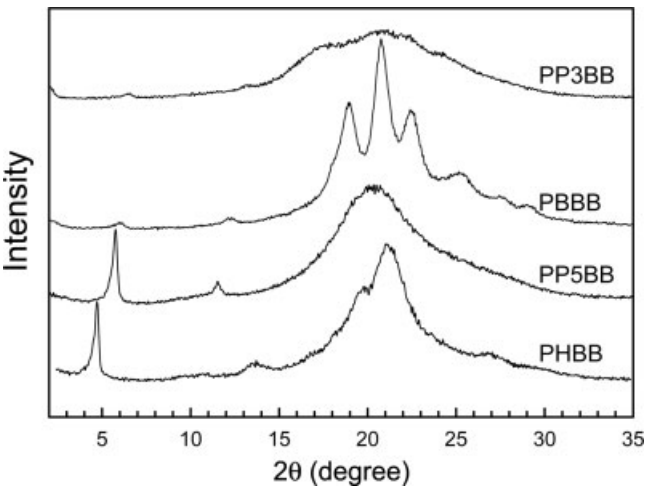

Figure 4 WAXD scans of quenched BB polyester films.

ΔH_{X-S}, which was followed by the S–I transition at T_{S-I} with an enthalpy of ΔH_{S-I}. The heating curve of PP3BB showed a single peak of the combined crystalline–smectic–isotropic transitions at 266°C. The total heat of 57 J/g equaled the sum of ΔH_{I-S} and ΔH_{S-X} released in the cooling curve. Shoulders on the peaks in the heating thermograms of PBBB and PHBB were due to transitions between crystal polymorphs.[18,19] For example, cooling at 10°C/min produced mostly the α form of PHBB.[9,18,19] The subsequent heating curve of PHBB showed the α-form/γ-form transition as a shoulder at 210°C on the sharp γ–smectic (γ–S) endothermic peak at 218°C. The endothermic S–I transition followed at 240°C.

The transition temperatures and transition enthalpies, plotted in Figure 2 as functions of the number of methylene units in the aliphatic diol (n), showed typical odd–even oscillations, with larger values observed in polyesters with even-numbered spacers.

Quenched BB polyesters

The thermograms in Figure 3 were obtained through the heating of compression-molded films that had been quenched from the isotropic melt. Quenched PP3BB, PBBB, and PHBB exhibited virtually the same X–S and S–I transitions as the slowly cooled specimens in Figure 1. The quenched PP5BB film exhibited a very broad cold crystallization peak in the 80–150°C temperature range, which was followed by the X–S and S–I transitions at the same temperatures shown in Figure 1. An absolute enthalpy of about 11.0 J/g for both cold crystallization and subsequent melting categorized the quenched PP5BB film as an LC glass without conventional crystallinity.

The WAXD patterns of the quenched films are shown in Figure 4. The crystallization of PP3BB during quenching from the isotropic state produced broad crystalline reflections at 17.3, 22.4, and 24.3°. The weak peak close to 6.55° with the second-order peak at 13.2° corresponded to the smectic layer spacing of 13.7 Å. The low intensity of the smectic layer reflection was probably due to disruption and distortion of the smectic layers during crystallization.[9] Quenched PBBB showed much stronger crystalline reflections at 19.0, 20.8, 22.4, 25.4, and 29.0°. The weak peak at 6.00° with the second-order peak at 12.1° corresponded to a spacing of 14.7 Å, which was significantly smaller than the smectic layer spacing reported for PBBB of 15.8 Å.[14] The low intensity and shifted spacing indicated that crystallization distorted the smectic layers.

In contrast, quenched PP5BB exhibited a sharp peak at 5.75° with a weaker second-order peak corresponding to a smectic layer spacing of 15.4 Å. The absence of crystalline reflections confirmed the finding from thermal analysis that the quenched PP5BB film was an LC

TABLE I
Oxygen–Barrier Properties of Polyesters Based on BB

Sample	Density (g/cm^3)	T_g from DSC (°C)	P [cc (STP) cm/m^2/atm/day][a]	D (10^{-13} m^2/s)	S [cc (STP)/cm^3/atm]	Layer spacing (Å)[b] Experimental	Layer spacing (Å)[b] Calcd	Hole size (Å)	ΔH_{total} (J/g)[c]	ϕ_w from WAXD	S_m [cc (STP)/cm^3/atm]
PP3BB	1.3154 ± 0.0004	—	0.040 ± 0.001	3.3 ± 0.3	0.014 ± 0.001	13.7	—	2.37	57	0.15	0.016
PBBB	1.3147 ± 0.0005	58[d]	0.022	3.7	0.0068	14.7	17.2	2.50	65	0.41	0.012
PP5BB	1.2699 ± 0.0012	30	0.0921 ± 0.0008	6.5 ± 0.1	0.0164 ± 0.0004	15.4	17.2	2.34	18	0	0.016
	1.2775 ± 0.0008[e]		0.0577 ± 0.0002[e]	5.1 ± 0.1[e]	0.0131 ± 0.0004[e]	15.2[e]	17.2[e]	—	34[e]	0.22[e]	0.017[e]
PHBB	1.2469 ± 0.0008	48	0.0906 ± 0.0008	7.3 ± 0.1	0.0141 ± 0.0001	18.8	19.6	2.48	57	0.29	0.020
PBBB-30I	1.2896 ± 0.0004	43	0.099 ± 0.001	4.6 ± 0.4	0.025 ± 0.001	—	—	2.47	28	0.31	0.036
PP5BB-30I	1.2426 ± 0.0006	28	0.314 ± 0.009	9.3 ± 0.3	0.0391 ± 0.0010	—	—	2.56	0	0	0.039
PP5BB-30I	1.2436 ± 0.0006	32	0.169 ± 0.009	8.4 ± 0.3	0.0232 ± 0.0021	—	—	2.54	35	0.18	0.039
PEOBB	1.3112 ± 0.0003	89	0.521 ± 0.002	5.9 ± 0.3	0.102 ± 0.004	—	—	2.59	0	0	0.102
PBOBB	1.2735 ± 0.0008	50	0.528 ± 0.002	10.1 ± 0.1	0.061 ± 0.001	—	—	2.57	0	0	0.061
PHOBB	1.2285 ± 0.0007	30	0.731 ± 0.002	21.4 ± 0.4	0.040 ± 0.001	—	—	2.61	0	0	0.040
PET[f]	1.3370 ± 0.0004	76	0.450	5.8	0.090	—	—	2.56	0	0	0.090

[a] 0.152 barrer.
[b] Reference 14.
[c] The sum of the enthalpy of cold crystallization and the enthalpies of the crystalline and smectic transitions.
[d] Estimated.
[e] Crystallized PP5BB (ref. 8).
[f] Reference 5.

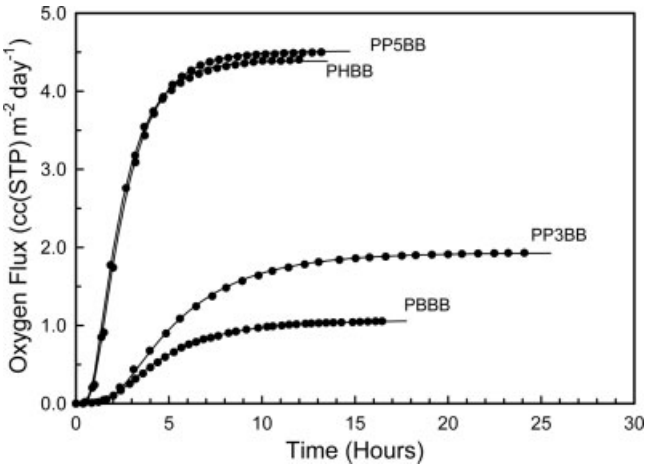

Figure 5 Experimental $J(t)$ data for quenched BB films tested at 23°C and fitted to eq. (1).

glass without conventional crystallinity. Several crystal forms exist for PHBB. When quenched from the isotropic melt, the PHBB film exhibited the γ form, as indicated by relatively weak reflections at 2θ values of 13.7, 19.7, and 21.2° in the WAXD pattern.[9,18,19] A sharp peak at 4.70° corresponded to the spacing of the smectic layers of 18.8 Å. The layer spacings of PP5BB and PHBB agreed with the literature reports for the smectic phase.[20] The layer spacing increased with the length of the diol spacer. However, the layer spacings were significantly less than the calculated length of the fully extended repeat unit of 17.2 Å for PBBB and PP5BB and of 19.6 Å for PHBB.[14] The difference was attributed to the presence of some gauche or eclipsed conformations of the spacer.[14,21]

The weight fraction of crystallinity (ϕ_w) estimated from the WAXD pattern is listed in Table I. The value of ϕ_w showed the same odd–even oscillation observed in the enthalpy. It increased from 0.15 for quenched PP3BB to 0.41 for quenched PBBB, decreased to 0 for quenched PP5BB, and increased again to 0.29 for quenched PHBB. The glass-transition temperature (T_g) and the total enthalpy (ΔH_{total}), defined as the sum of the enthalpy of cold crystallization and the enthalpies of the crystalline and smectic transitions, are also compiled in Table I.

Oxygen-transport properties

Typical experimental curves in Figure 5 describe $J(t)$ through PP3BB, PBBB, PP5BB, and PHBB at 23°C. The flux curves were normalized to a film thickness of 200 μm to facilitate comparisons among specimens that varied somewhat in thickness. Careful conditioning and the appropriate choice of the specimen thickness resulted in excellent resolution of the various features of the time dependence. The initial increase in $J(t)$ reflected non-steady-state diffusion. This part of the curve was controlled mainly by D. As the permeant concentration in the specimen reached a constant distribution, the flux reached the steady-state value (J_0). This value, normalized to l and p, defined P as $P = J_0 l p^{-1}$.

A comparison of the flux curves indicated that an increase in the spacer length affected both the non-steady-state and steady-state parts of the flux curve. The fit to the solution of Fick's second law [eq. (1)] is included with the experimental points in Figure 5. The fit was equally good for all the experiments in the study. The two fitting parameters, P/l and D/l^2, were

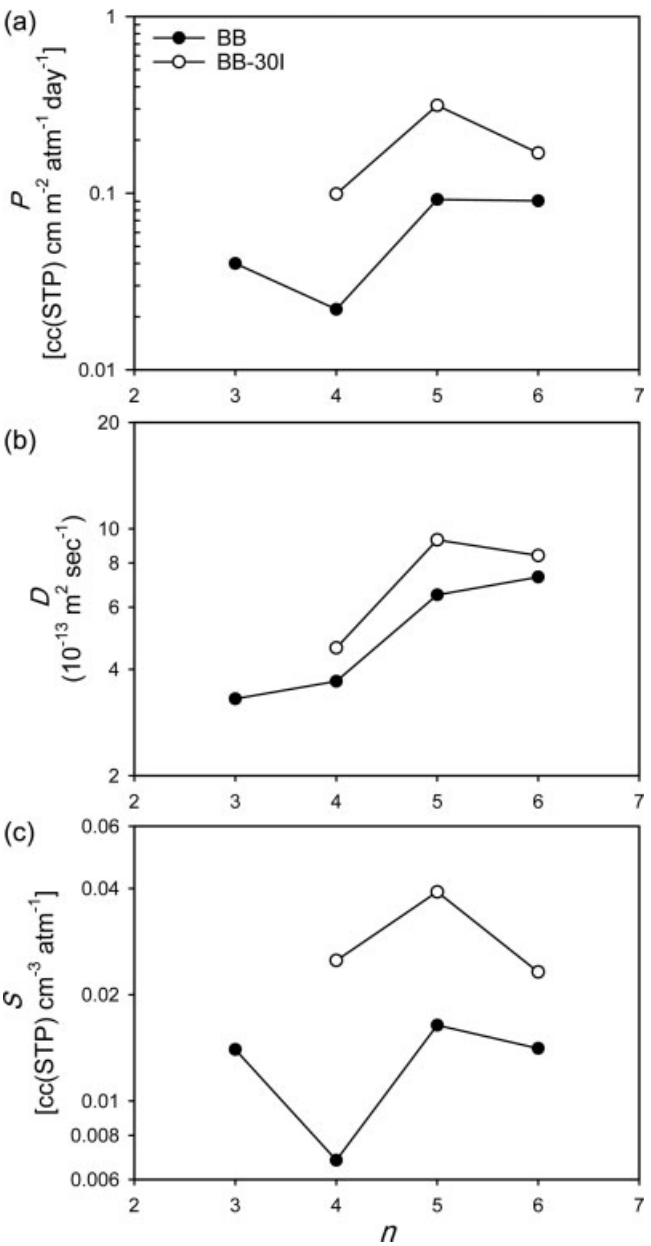

Figure 6 Effect of spacer length n on the oxygen-transport parameters of quenched BB and BB-30I polyester films at 23°C: (a) P, (b) D, and (c) S.

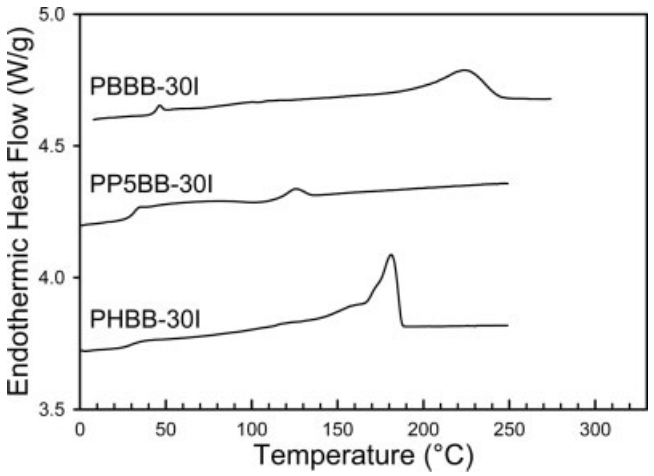

Figure 7 Heating thermograms of quenched BB-30I copolyester films.

used to obtain D and to accurately determine P. S was calculated with the relationship $S = PD^{-1}$.

The oxygen barrier properties at 23°C are plotted as a function of the spacer length in Figure 6. The oxygen permeability and solubility showed an odd–even effect, whereas D increased steadily as n increased. The low P and S values of PBBB and PHBB, which produced the odd–even effect, were possibly the result of crystallization. Although the quenched PP5BB was an LC glass, it is known to crystallize upon annealing at elevated temperatures.[8] Values from the literature for P, D, and S of crystallized PP5BB are included in Table I. When the lower values of P and S were considered, the odd–even effect for PP5BB was lost. The differences in the chain conformations of the BB polyesters with odd and even spacers, which caused the dramatic odd–even effect in the thermal transitions, possibly did not alter the glassy regions enough to produce a similar odd–even effect in the gas-transport properties.

The lowest P value was 0.022 cc (STP) cm m^{-2} day^{-1} atm^{-1} for PBBB, which was more than 20 times lower than P of glassy poly(ethylene terephthalate) (PET), which was 0.450 cc (STP) cm m^{-2} day^{-1} atm^{-1}. The P value of PBBB was comparable to that of another aromatic LC polyester with an aliphatic diol, poly(ethylene terephthalate-*co*-*p*-hydroxybenzoate), but an order of magnitude higher than P of a wholly aromatic LC polyester, poly(*p*-hydroxybenzoate-*co*-*p*-hydroxynaphthalate).[5] The very low oxygen permeability of the BB polyesters and other LCPs resulted mainly from very low gas solubility.

Copolyesters with isophthalic acid

The thermograms of copolymers with 30 mol % BB replaced with nonmesogenic isophthalic acid are shown in Figure 7. The thermograms show a well-defined glass transition and a broad melting endotherm at higher temperatures. In general, copolymerization reduced the transition temperatures, including T_g. The thermograms did not exhibit distinct X–S and S–I transitions as the thermograms of the homopolymers did.

The WAXD pattern of quenched PBBB-30I in Figure 8 shows the same crystalline reflections as PBBB did at 19.0, 20.8, 22.4, and 25.4° (Fig. 4), and this indicated that the isophthalate unit was excluded from the PBBB crystal lattice. A reflection corresponding to the smectic layer spacing was barely discernable at about 6°. If PBBB-30I retained some LC character, the broad endotherm of PBBB-30I would have encompassed both the X–S and S–I transitions.

The heating thermogram of quenched PP5BB-30I showed a small cold crystallization peak at 105°C and a subsequent melting peak at 127°C. An absolute enthalpy of about 0.1 J/g for both cold crystallization and subsequent melting indicated that quenched PP5BB-30I was a glass. This was confirmed by the broad, amorphous reflection in WAXD.

It has been reported that PHBB-30I possesses some LC character.[9] The complex endothermic peak in the heating curve of PHBB-30I at about 180°C would have encompassed the α–γ, γ–S, and S–I transitions. WAXD of quenched PHBB-30I showed poorly defined α-form reflections at 18.1 and 24.3° superimposed on a broad, amorphous peak. The reflection corresponding to the smectic layer spacing was not detected. It is known that the smectic layer spacing is very weak in the α form of PHBB.[9] This may be because the α form has the fully extended chain conformation with a fiber repeat of 19.62 Å and a unit cell density of 1.307 g/cm^3, whereas the chain conformation in the γ form, with a shorter fiber repeat of 19.39 Å and a lower unit cell density of 1.254 g/cm^3, is closer to that of the smectic

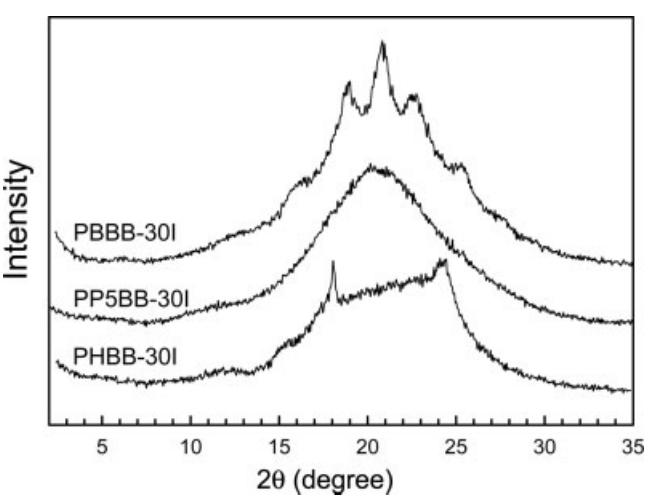

Figure 8 WAXD scans of quenched BB-30I copolyester films.

form with a layer spacing of 18.8 Å.[19] Consequently, it may be possible for the γ form to coexist with the smectic phase, whereas transformation to the α form requires larger axial shifts that disrupt the smectic order.

The estimated values of ϕ_w, based on the WAXD patterns, are listed in Table I. ϕ_w decreased with the incorporation of isophthalic acid from 0.41 for PBBB to 0.31 for PBBB-30I. A similar decrease in ϕ_w was observed for PHBB and PHBB-30I. The values of T_g and ΔH_{total} for the copolymers are compiled in Table I.

The incorporation of 30 mol % isophthalic acid increased P considerably, by a factor of about 4 (Fig. 6). The higher P values of the copolyesters were due to increases in both D and S, with a slightly larger percentage increase in S. Copolymerization reduced the LC order and also reduced the crystallinity of PBBB and PHBB. Both factors were expected to increase P. However, the reduced LC character probably had a somewhat larger effect.

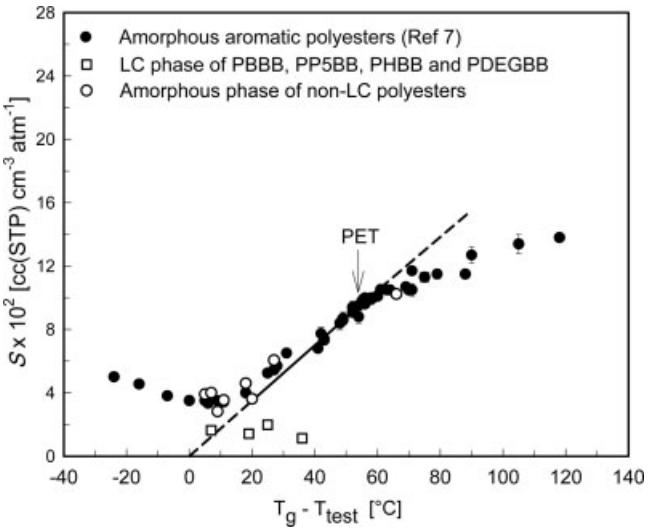

Figure 9 Relationship between S and $T_g - T_{\text{test}}$. The data represented by the solid symbols were taken from ref. 7. The data for poly(diethylene glycol 4,4′-bibenzoate) (PDEGBB) were taken from ref. 5.

Polyesters with OBB

The polyesters based on BB were also compared with aromatic polyesters synthesized from aliphatic diols with an even number of carbon atoms and a diacid that differed from BB by having the phenyl groups separated by an ether oxygen (OBB). All the quenched OBB polymers were amorphous, as indicated by thermal analysis and WAXD. A lower T_g compared with that of the corresponding BB polyester reflected the additional flexibility imparted by the ether group (Table I).

The oxygen-transport properties were typical for amorphous aromatic polyesters such as PET (Table I). D increased with the number of carbon atoms in the aliphatic spacer, and S decreased as T_g approached the ambient temperature. The effects were largely offsetting, so P increased only somewhat with the length of the aliphatic spacer.

Oxygen sorption and free volume

The interpretation of the transport parameters obtained at 23°C was complicated by the proximity of the test temperature (T_{test}) to the polymer T_g, at which major changes in the mechanism of gas transport occur. The effect of the glass transition on oxygen solubility is shown in Figure 9, which shows a plot of S as a function of T_{test} with respect to T_g ($T_g - T_{\text{test}}$).[9] Data from the literature for numerous amorphous aromatic polyesters are included, so the plot covers a large range of $T_g - T_{\text{test}}$ and encompasses T_g.[7] In the glassy state, as reflected by the right branch in Figure 9, oxygen sorption at a low pressure is the process of filling holes of excess free volume.[22–24] The amount of excess hole free volume decreases as the temperature approaches T_g. This appears in Figure 9 as a linear relationship between S and $T_g - T_{\text{test}}$, which extrapolates to zero solubility at $T_{\text{test}} = T_g$, at which the excess free volume is expected to disappear.[25] The slope gives the density of the sorbed oxygen in the free-volume holes.[22] Further from T_g, the decreasing slope indicates that the free volume approaches a constant value above the second-order transition at $T_g - 60$°C.[22] As T_{test} approaches T_g, the contribution of Henry's law sorption is responsible for the deviation from the linear relationship. The oxygen solubility gradually increases as the polymer reaches the rubbery state, and this is reflected by the left branch in Figure 9.

It is possible to extract the oxygen solubility in the noncrystalline regions of BB and BB-30I polyesters from the measured values if we consider the effect of crystallinity. The two-phase solubility model considers an impermeable crystalline phase dispersed in a permeable noncrystalline matrix:

$$S = S_m(1 - \phi_c) \tag{2}$$

where S_m is the oxygen solubility of the noncrystalline LC or amorphous phase and ϕ_c is the volume fraction of crystallinity. With the crystallinity estimated from WAXD, S_m was calculated with eq. (2) and is listed in Table I.

The results are included in Figure 9, with T_g measured from differential scanning calorimetry. The solubility of oxygen in the noncrystalline regions of the BB-30I copolyesters and in the amorphous OBB polyesters conformed to the relationship between S and $T_g - T_{\text{test}}$ established for amorphous glassy and rub-

bery aromatic polyesters. This was consistent with the interpretation that the noncrystalline phase did not possess LC character even though PBBB-30I and PHBB-30I might have crystallized from the partially LC melt.[9] On the other hand, S_m for the LC polyesters was lower than expected on the basis of the amorphous polyesters and was essentially independent of the spacer length (Table I). The low solubility of the noncrystalline LC phase was ascribed to the smaller free-volume hole size and possibly to the lower free-volume hole density in comparison with an amorphous glass.[7]

CONCLUSIONS

BB polyesters are especially attractive for the investigation of structure–property relationships of LCPs because they can be prepared in conventional polyester reactors and can be readily molded as films with good mechanical properties. A strong odd–even effect of the aliphatic spacer length was demonstrated for the thermal transitions of the BB polyesters. However, the effect was weak or absent from the oxygen-transport properties when the effect of crystallinity was considered. The oxygen permeability and diffusivity showed an increasing trend with the spacer length. Estimates of the oxygen solubility in the noncrystalline LC phase, based on a simple two-phase model, revealed that the oxygen solubility was almost independent of the spacer length. In contrast, the oxygen solubility in the non-LC BB-30I copolyesters and OBB polyesters conformed to the relationship between S and T_g previously established for amorphous and glassy aromatic polyesters. Comparisons between LC and non-LC polyesters confirmed that low oxygen solubility was responsible for the low permeability of LC polyesters. The low solubility of the noncrystalline LC phase was ascribed to a smaller free-volume hole size and possibly to a lower free-volume hole density compared with those of an amorphous glass.

Modern Controls, Inc., generously supported the development of a facility for gas-transport studies at Case Western Reserve University.

References

1. Chiou, J. S.; Paul, D. R. J Polym Sci Part B: Polym Phys 1987, 25, 1699.
2. Weinkauf, D. H.; Paul, D. R. J Polym Sci Part B: Polym Phys 1991, 29, 329.
3. Weinkauf, D. H.; Paul, D. R. J Polym Sci Part B: Polym Phys 1992, 30, 817.
4. Weinkauf, D. H.; Paul, D. R. J Polym Sci Part B: Polym Phys 1992, 30, 837.
5. Hu, Y. S.; Schiraldi, D. A.; Hiltner, A.; Baer, E. Macromolecules 2003, 36, 3606.
6. Hu, Y. S.; Liu, R. Y. F.; Schiraldi, D. A.; Hiltner, A.; Baer, E. Macromolecules 2004, 37, 2128.
7. Hu, Y. S.; Liu, R. Y. F.; Schiraldi, D. A.; Hiltner, A.; Baer, E. Macromolecules 2004, 37, 2136.
8. Hu, Y. S.; Hiltner, A.; Baer, E. Polymer 2006, 47, 4058.
9. Hu, Y. S.; Hiltner, A.; Baer, E. Polymer 2006, 47, 2423.
10. Jackson, W. J. Jr; Morris, J. C. In Liquid-Crystalline Polymers; Weiss R. A.; Ober C. K., Eds., American Chemical Society: Washington, DC, 1990, Chapter 2, p 16.
11. Watanabe, J.; Hayashi, M.; Nakata, T.; Niori, T.; Tokita, M. Prog Polym Sci 1997, 22, 1053.
12. Krigbaum, W. R.; Asrar, J.; Toriumi, H.; Ciferri, A.; Preston, J. J Polym Sci Polym Lett Ed 1982, 20, 109.
13. Meurisse, P.; Noel, C.; Monnerie, L.; Fayolle, B. Br Polym J 1981, 13, 55.
14. Watanabe, J.; Hayashi, M. Macromolecules 1988, 21, 278.
15. Nakata, Y.; Watanabe, J. Polym J 1997, 29, 193.
16. Higuchi, H.; Yu, Z.; Jamieson, A. M.; Simha, R.; McGervey, J. D. J Polym Sci Part B: Polym Phys 1995, 33, 2295.
17. Sekelik, D. J.; Stepanov, S. V.; Nazarenko, S.; Schiraldi, D.; Hiltner, A.; Baer, E. J Polym Sci Part B: Polym Phys 1999, 37, 847.
18. Krigbaum, W. R.; Watanabe, J. Polymer 1983, 24, 1299.
19. Li, X.; Brisse, F. Macromolecules 1994, 27, 7725.
20. Watanabe, J.; Hayashi, M. Macromolecules 1988, 21, 4083.
21. Abe, A. Macromolecules 1984, 17, 2280.
22. Polyakova, A.; Liu, R. Y. F.; Schiraldi, D. A.; Hiltner, A.; Baer, E; Baer, E. J Polym Sci Part B: Polym Phys 2001, 39, 1889.
23. Hiltner, A.; Liu, R. Y. F.; Hu, Y.; Baer, E. J Polym Sci Part B: Polym Phys 2005, 43, 1047.
24. Weiss, G. H.; Bendler, J. T.; Shlesinger, M. F. Macromolecules 1992, 25, 990.
25. Vrentas, J. S.; Duda, J. L; Shlesinger, M. F. J Appl Polym Sci 1978, 22, 2325.